The influence of substrate polarity on the structural quality of InN layers grown by high-pressure chemical vapor deposition

N. Dietz,[1,a] M. Alevli,[1] R. Atalay,[1] G. Durkaya,[1] R. Collazo,[2] J. Tweedie,[2] S. Mita,[2] and Z. Sitar[2]
[1]*Department of Physics and Astronomy, Georgia State University, Atlanta, Georgia 30302-4106, USA*
[2]*Department of Materials Science and Engineering, North Carolina State University, Raleigh, North Carolina 27695-7919, USA*

(Received 11 December 2007; accepted 14 January 2008; published online 31 January 2008)

The influence of substrate polarity on the properties of InN layers grown by high-pressure chemical vapor deposition has been studied. The 2Θ-ω x-ray diffraction scans on InN layers deposited on polar GaN epilayers revealed single-phase InN(0002) with a full width at half maximum (FWHM) of around 200 arc sec. InN layers grown on N-polar GaN exhibit larger FWHMs. Rocking curve analysis confirmed single-phase InN for both growth polarities, with FWHM values for ω-RC(002) at 2080 arc sec for InN grown on Ga-polar templates. The A_1(LO) Raman mode analysis shows higher free carrier concentrations in InN grown on N-polar templates, indicating that polarity affects the incorporation of impurities. © *2008 American Institute of Physics*. [DOI: 10.1063/1.2840192]

The optimization of InN and indium-rich group III-nitride alloys is of crucial importance for indium-rich group III-nitride alloys in advanced device structures for solid-state lighting, photovoltaics, spintronics, and terahertz[1] applications utilizing the large spectral tunability and multifunctionality of group III-nitride alloys. The embedding of InN and indium-rich group III-nitride alloys into wide band gap group III-nitride compound semiconductors (e.g., GaN and AlN) is essential for the successful fabrication of spectral tunable light sources and highly efficient photovoltaic converters.[2] A key issue is to understand and establish the physical properties of InN and how they relate to indium-rich group III-nitride alloys since some properties still vary strongly with the process conditions applied.[3] At present, the large thermal decomposition pressure of InN and indium-rich group III-nitride limits the growth temperatures to below 650 °C for low-pressure metal organic chemical vapor deposition (MOCVD) and molecular beam epitaxy growth processes. However, the integration of indium-rich group III-nitride layers into $Ga_{1-x}Al_xN$ alloys strongly depends on the *existence of overlapping processing windows* as well as on the precise control of the thermal decomposition pressures and stoichiometry of indium-rich alloys at the optimum processing temperatures.

To overcome thermodynamic constraints—formulated for equilibrium processes—clever off-equilibrium processes that allow the stabilization of indium-rich group III-nitride alloys at low pressures and result in improved optical and structural qualities of the layers have been developed.[4] However, these approaches are problematic due to large thermal decomposition pressure at the optimum growth temperature, creating conflicting material properties. Moreover, the integration of indium-rich alloys with wide band gap group III-nitride alloys remains an unsolved problem, restricting the development of potential advanced device structures. Surface stabilization data have shown that InN can be grown at much higher temperatures if stabilized at high nitrogen pressures,[5,6] evoking the development of the high-pressure chemical vapor deposition (HPCVD) system,[7,8] capable of operating at reactor pressures up to 100 atm. This approach provides a control of vast constituents with different partial pressures, which may enable the fabrication of indium-rich group III-nitrides. The details of the HPCVD system has been described elsewhere.[9]

The InN layers were grown by HPCVD, employing ammonia (NH_3) and trimethylindium (TMI) as precursors. A pulsed injection scheme utilizing pulse width, precursor pulse separation, and cycle sequence time as control parameters was followed in order to control the gas phase and surface chemistry kinetics. For the layers described below, the reactor pressure was 15 bars, the total gas flow 12 slm (standard liters per minute), the precursor molar ratio ammonia to TMI 600, and the growth temperature 850 °C. The different polar GaN layers were grown by low-pressure MOCVD on sapphire substrates to a thickness of 1.5 μm. The growth and identification procedure has been described elsewhere.[10,11] The GaN templates did not receive any further treatment prior to the InN layer growth. No buffer layer was used for the growth of InN on the Ga- and N-polar templates.

Crystallographic characterization was performed by acquiring on- and off-axis high-resolution x-ray diffraction ω-rocking curves and 2Θ-ω scans using a Philips X'Pert MRD with a copper x-ray source. An open slit on the detector side in the double axis configuration was used for the ω-rocking curves, while a triple axis configuration was used for the 2Θ-ω scans perpendicular to the sample surface. The full widths at half maximum (FWHMs) of the (002) symmetric reflection and the (302) skew-symmetric reflection for the N-polar GaN were 774 and 1395 arc sec, respectively, and those for the Ga-polar GaN were 410 and 1386 arc sec, respectively. The observed difference between the FWHMs of the ω-rocking curves of the two films is attributed to the absence of the low-temperature AlN nucleation layer on the N-polar films, following the polarity control scheme.

Figure 1 shows a 2Θ-ω scan for the InN film grown on Ga-polar GaN (209L) that includes three Bragg peaks corre-

[a]Author to whom correspondence should be addressed. Electronic mail: ndietz@gsu.edu.

Author complimentary copy. Redistribution subject to AIP license or copyright, see http://apl.aip.org/apl/copyright.jsp

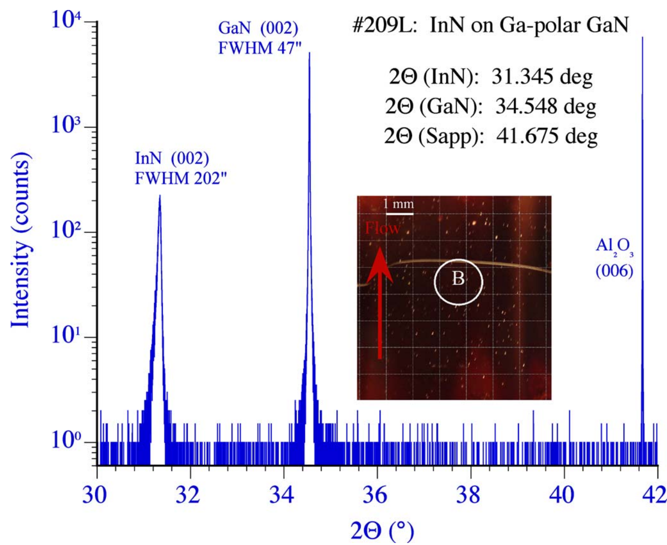

FIG. 1. (Color online) 2Θ-ω XRD scan in triple crystal geometry for InN layer 209L-B grown on Ga-polar GaN/sapphire template. The inset shows a section of the InN sample and the location analyzed.

TABLE I. Structural data for InN layers grown on N- and Ga-polar GaN templates.

		Sample 207L InN on N-polar GaN	Sample 209L InN on Ga-polar GaN
XRD:	2Θ-InN(002) position	31.311°	31.345°
	2Θ-InN(002) FWHM	295 arc sec	202 arc sec
	ω-RC(002) FWHM	4243 arc sec	2082 arc sec
	ω-RC(103) FWHM	5000 arc sec	2857 arc sec
	ω-RC(302) FWHM	6100 arc sec	3501 arc sec
Raman:	E_2(high) position	487.7 cm^{-1}	486.3 cm^{-1}
	E_2(high) FWHM	9.4 cm^{-1}	8.3 cm^{-1}
	A_1(LO) position	593.1 cm^{-1}	591.9 cm^{-1}
	A_1(LO) FWHM	20.8 cm^{-1}	18.2 cm^{-1}
ε_∞ [via A_1(LO) simulation]		7.9	7.8
Free carrier concentration [via A_1(LO) simulation]		4.3×10^{18}	2.5×10^{18}
d_{InN} (from transmission)		470 nm	470 nm
Absorption band edge		1.23 eV	1.21 eV

sponding to the InN(002), GaN(002), and sapphire (006) reflections. Figure 2(a) shows the InN(002) Bragg peak, along with the peaks resulting from a deconvolution procedure using Gaussian peaks. The Bragg peak is composed of two peaks, a sharp dominant peak corresponding to InN and a secondary peak at a lower angle with an area ratio and a height ratio between the main peak and the secondary peak of 1.3 and 3.2, respectively. The ω-rocking curves for the InN symmetric (002) and skew-symmetric (103) and (302) reflections are shown in Fig. 2(b). The FWHMs of these curves are summarized in Table I, along with other pertinent crystallographic information. The x-ray diffraction (XRD) analysis for the symmetric and skew-symmetric reflections indicates that InN grew in a single phase and epitaxially on the GaN template.

It is interesting to contrast the results from the InN layer grown on a Ga-polar template with those obtained from a layer grown on a N-polar GaN template (207L). Similar to 209L, the 2Θ-ω scan performed on the layer grown on a N-polar template does not show any other reflections besides those already listed. Comparing the positions of the InN(002) Bragg peaks, a shift of the peak corresponding to 207L toward lower angles was observed. Also, as the InN layer grown on the Ga-polar template, the Bragg peak is composed of two peaks with an area ratio and a height ratio between the main peak and the secondary peak of 0.95 and 2.4, respectively. Although this secondary peak is more prominent in the layer grown on the N-polar template than in the layer grown on the Ga-polar template, its nature is difficult to assess. The secondary peak may represent a secondary phase, or a strain state due to biaxial stresses, the presence of native point defects, or impurity incorporation.

In addition, the FWHMs of the 207L ω-rocking curves are twice those for 209L, suggesting a decrease in the crystalline quality of the sample with respect to the layer grown on a Ga-polar GaN template. InN layer etching using 3*M* KOH solution at 65 °C for 10 min shows no selective etching of the surface, which would suggest an In-polar surface. Further etching with a stronger 10*M* KOH solution revealed nonselective etching; however, the etched features for the InN layer grown on N-polar GaN were much larger in number and size. This could be due to the either different starting

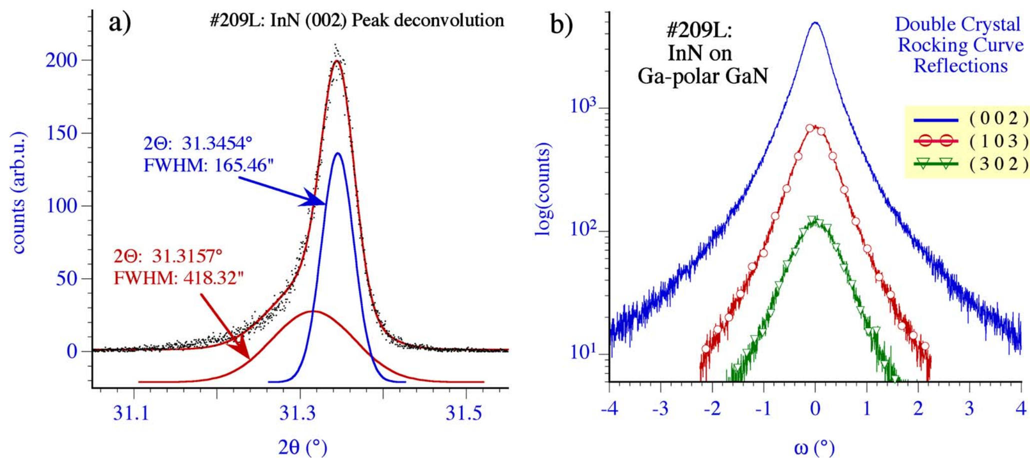

FIG. 2. (Color online) (a) The InN peak deconvolution indicates an asymmetric lower shoulder, which might be due to impurities. (b) Rocking curve analysis of the higher order InN peaks: (i) ω-RC(002), peak position ω=15.7725° with FWHM=2082 arc sec; (ii) ω-RC(103), peak position ω=28.5241° with FWHM=2857 arc sec; and (iii) ω-RC(302), peak position ω=53.2070° with FWHM=3501 arc sec.

Author complimentary copy. Redistribution subject to AIP license or copyright, see http://apl.aip.org/apl/copyright.jsp

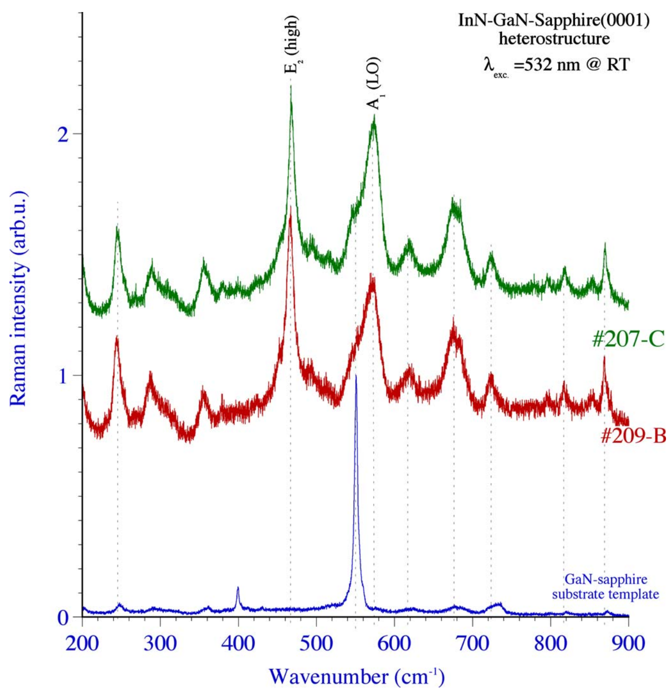

FIG. 3. (Color online) Raman spectra for InN layers 207L and 209L grown on N-polar and Ga-polar GaN/sapphire templates, respectively.

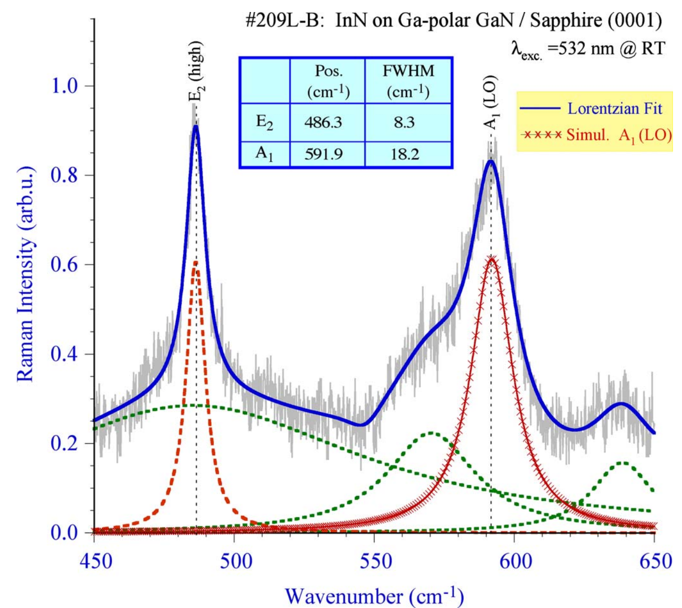

FIG. 4. (Color online) Analysis of E_2(high) and A_1(LO) modes in Raman spectrum for InN layer 209L grown on Ga-polar GaN/sapphire template.

surface morphology or the higher defect incorporation.

Figure 3 shows the Raman spectra for the InN layers grown on N-polar and Ga-polar GaN/sapphire substrates in the energy range of 200–900 cm^{-1}. The spectra are taken in the backscattering geometry $z(\cdots)z$ using an excitation energy of 2.33 eV at room temperature. The observed E_2(high) and A_1(LO) peak positions are in good agreement with predicted phonon frequencies of 486 and 591 cm^{-1}, respectively, as reported by Davydov and Klochikhin.[12] To analyze the structural quality as well as the free carrier concentration in these layers, the two optical phonon modes of hexagonal InN, E_2(high) and A_1(LO), have been analyzed in more detail. Due to the nonpolar character of the E_2(high) mode, there is no interaction of this mode with the conduction-band electrons.[13] On the other hand, the A_1(LO) mode strongly interacts with the conduction-band electrons, and the magnitude of this interaction depends on the free electron concentration.[14,13]

In order to calculate the free carrier concentration quantitatively, the line shape of A_1(LO) was simulated using the Linhard–Mermin dielectric function, taking into account finite wave-vectors, for the deformation potential electro-optic scattering mechanism. The effective mass m_{eff} was kept constant at $0.14m_0$, noting that this will slightly underestimate the free carrier concentration.[15] The best-fit approximation for sample 209L is presented in Fig. 4, with the corresponding simulation results summarized in Table I. The band gap energy of the InN layers has been obtained from optical transmission measurements. The transmission spectra have been fitted by applying a modified model sielectric function.[16] The best-fit parameter values provide the parameters for thickness, high-frequency dielectric constant, and optical absorption edge.

In conclusion, we have analyzed the structural properties of InN layers grown by HPCVD on polarity controlled GaN/sapphire substrate templates. The XRD analysis revealed epitaxial, single-phase InN(0002) layers with hexagonal symmetry and a FWHM of the 2Θ-ω scan of around 200 arc sec for layers deposited on Ga-polar GaN epilayers. The FWHM increases for InN layers grown on N-polar GaN templates, using the same growth conditions. The free carrier concentrations in these InN layers were estimated by A_1(LO) line shape analysis and determined in the low 10^{18} cm^{-3}. The results suggest that the polarity of the substrate surface affects the defect incorporation during the growth and the subsequent structural and electrical properties of the InN layers.

This work was supported by AFOSR Grant No. FA9550-07-1-0345.

[1]G. D. Chern, E. D. Readinger, H. Shen, M. Wraback, C. S. Gallinat, G. Koblmuller, and J. S. Speck, Appl. Phys. Lett. **89**, 141115 (2006).
[2]K. S. A. Butcher and T. L. Tansley, Superlattices Microstruct. **38**, 1 (2005).
[3]D. Alexandrov, K. Scott, A. Butcher, and T. L. Tansley, J. Cryst. Growth **288**, 261 (2006).
[4]J. Wu, W. Walukiewicz, K. M. Yu, J. W. Ager III, E. E. Haller, H. Lu, W. J. Schaff, Y. Saito, and Y. Nanishi, Appl. Phys. Lett. **80**, 3967 (2002).
[5]B. Onderka, J. Unland, and R. Schmid-Fetzer, J. Mater. Res. **17**, 3065 (2002).
[6]J. MacChesney, P. M. Bridenbaugh, and P. B. O'Connor, Mater. Res. Bull. **5**, 783 (1970).
[7]M. Alevli, G. Durkaya, W. Fenwick, A. Weerasekara, V. Woods, I. Ferguson, A. G. U. Perera, and N. Dietz, Appl. Phys. Lett. **89**, 112119 (2006), and references therein.
[8]V. Woods and N. Dietz, Mater. Sci. Eng., B **127**, 239 (2006).
[9]N. Dietz, in *III-Nitrides Semiconductor Materials*, edited by Z. C. Feng (Imperial College, London, 2006), Chap. 6, pp. 203–235.
[10]R. Collazo, S. Mita, A. Aleksov, R. Schlesser, and Z. Sitar, J. Cryst. Growth **287**, 586 (2006).
[11]R. Collazo, S. Mita, R. Schlesser, and Z. Sitar, Phys. Status Solidi C **2**, 2117 (2005).
[12]V. Yu. Davydov and A. A. Klochikhin, Semiconductors **38**, 861 (2004).
[13]J. S. Thakur, D. Haddad, V. M. Naik, R. Naik, G. W. Auner, H. Lu, and W. J. Schaff, Phys. Rev. B **71**, 115203 (2005).
[14]F. Demangeot, C. Pinquier, J. Frandon, M. Gaio, O. Briot, B. Maleyre, S. Ruffenach, and B. Gil, Phys. Rev. B **71**, 104305 (2005).
[15]P. Rinke, M. Scheffler, A. Qteish, M. Winkelnkemper, D. Bimberg, and J. Neugebauer, Appl. Phys. Lett. **89**, 161919 (2006).
[16]T. Kawashima, H. Yoshikawa, S. Adachi, S. Fuke, and K. Ohtsuka, J. Appl. Phys. **82**, 3528 (1997).

Author complimentary copy. Redistribution subject to AIP license or copyright, see http://apl.aip.org/apl/copyright.jsp